Molecular Plant Breeding 2023, Vol.14, No.16, 1-11
http://genbreedpublisher.com/index.php/mpb

Research Article Open Access

# ZmIQD27 Interacts with ZmCaMs and ZmKLCRs in Maize

Yongmeng Gao, Jun Xie, Xiaoduo Lu, Haiyan Li
National Engineering Laboratory of Crop Stress Resistance, School of Life Science, Anhui Agricultural University, Hefei, 230036, China
Corresponding author email: lihy@ahau.edu.cn

Molecular Plant Breeding, 2023, Vol.14, No.16 doi: 10.5376/mpb.2023.14.0016
Received: 07 Jun., 2023
Accepted: 19 Jul., 2023
Published: 04 Aug., 2023



**Preferred citation for this article**:
Gao Y.M., Xie J., Lu X.D., and Li H.Y., 2023, ZmIQD27 interacts with ZmCaMs and ZmKLCRs in maize, Molecular Plant Breeding, 14(16): 1-11 (doi: 10.5376/mpb.2023.14.0016)

**Abstract** Plant secondary cell wall (SCW) provides physical support for upright growth and the transportation of water and nutrients. In our previous report, we characterized ZmIQD27, an SCW development-related protein, colocalized with microtubules and its loss of function would result in upward water-transportation failure. While the molecular mechanism of how ZmIQD27 mediates microtubular arrangement was not addressed. In this paper, a ZmCaM-ZmIQD27-ZmKLCR cascade was identified in maize. Interactions between ZmIQD27 and ZmCaMs and ZmKLCRs were verified in vivo and in vitro. ZmIQD27 motif that is responsible for binding CaMs and KLCRs was characterized. A proposed model of ZmIQD27 acts as a scaffold protein that senses signals and mediates the SCW transportation on microtubules guided by kinesin, was proposed. Our results would be essential for enriching the molecular network of how ZmIQD27 modulates secondary cell wall development, which would finally help in marker-assisted maize breeding.

**Keywords** Secondary cell wall; ZmIQD27; ZmCaM; ZmKLCR; Interaction

## Introduction

The plant cell wall has a primary cell wall (PCW) and a secondary cell wall (SCW). The PCW forms when a cell divides. SCW forms between the cellular plasma membrane and PCW in specific cell types, such as epidermic cells that offer mechanical support and xylem vessel elements that conduct water and nutrients. Both PCW and SCW contain cellulose, hemicellulose, and pectin, while the latter contains a variable amount of lignin.

The common feature of IQD proteins is the presence of a central region of 67 conserved amino acid residues, referred to as the IQ67 domain. Diverse biological functions of IQD proteins have been reported (Abel et al., 2005; Abel et al., 2013; Feng et al., 2014; Ma et al., 2014; Bürstenbinder et al., 2013; 2017a; 2017b; Wu et al., 2016; Bi et al., 2018; Yuan et al., 2019; Liu et al., 2020; Li et al., 2021; Mei et al., 2021). Novel functions of IQDs on the production of biomass and cell wall chemistry were reported (Badmi et al., 2018). In Arabidopsis, loss-of-function of *Atiqd5* lines showed changed morphogenesis of pavement cell (PC) shape (Mitra et al., 2019).

ZmIQD27 was the first IQD protein that was reported to have functions in mediating SCW development in maize. There are at least 27 IQDs in maize, 26 of which were reported by Cai et al. (2016). ZmIQD27, the mutated gene of a drought-sensitive maize mutant screened from an EMS-induced mutant library of maize B73 (Lu et al., 2008), was characterized. ZmIQD27 functions by colocalizations with microtubules. The drought-sensitive phenotype of the mutant was due to defects of metaxylem vessels (Li et al., In press). A putative function of ZmIQD27 in SCW patterns consistent with that of AtIQD13 (Oda and Hasezawa, 2006; Oda et al., 2010; Oda and Fukuda, 2012; Oda et al., 2013a; 2013b; Sugiyama et al., 2017). Detailed molecular mechanism of how ZmIQD27 modulates microtubules and its loss-of-function leads to a disorder arrangement of microtubules, was not revealed.

A CaM-IQD-KLCR cascade was characterized in Arabidopsis (Abel et al., 2013; Bürstenbinder et al., 2013; 2017a; 2017b). IQD proteins belong to the family of CaM/CML-binding proteins. Calmodulin (CaM) and closely related CaM-like (CML) proteins are principal sensors of dynamic intracellular calcium ($Ca^{2+}$) fluctuations. CaM binding was detected in the absence of $Ca^{2+}$. The IQ67 domain mediates CaM binding in vitro (Bürstenbinder et al., 2013). In Arabidopsis, AtIQD1 interacts with CaM1, CaM2, CML8, and CML9 by pull-down assay (Bürstenbinder et al., 2013). IQD1 interacts with CaM1, CaM2, and CaM6, while IQD20 interacts with CaM2 and CML13 (Bürstenbinder et al., 2013).

Kinesins are a class of microtubule-based molecular motors that are usually hetero-tetrameric, consisting of two heavy chains (KHC) and two light chains (KLC) subunits, and facilitate directional transport of organelles, vesicles, multiprotein or ribonucleoprotein complexes to specific cellular destinations, generally toward the cell periphery. Kinesin light chain-related-1 (KLCR1) is a novel class of protein that interacts with IQDs. Three KLCRs from Arabidopsis, named KLCR1-3, were cloned and subjected to yeast two-hybrid (Y2H) assay. KLCR1 interacts with IQD1 (Bürstenbinder et al., 2013). In vivo, the binding of KLCR1 to IQD1 was confirmed in yeast and in plants. GFP-tagged IQD1 localized to microtubules, while expressed RFP-tagged KLCR1 displayed diffuse cellular fluorescence, indicative of cytosolic localization (Bürstenbinder et al., 2013). When co-transfected, RFP-tagged KCLR1 colocalized with the microtubular pattern of GFP-tagged IQD1 fluorescence, indicating the recruitment of RFP-tagged KLCR1 to the microtubular network by GFP-tagged IQD1 (Bürstenbinder et al., 2013). However, there are no CaMs or ZmKLCRs found interacting with ZmIQD27 in maize, there is no such a "ZmCaM-ZmIQD-ZmKLCR" cascade characterized in maize.

In this paper, ZmCaMs, and ZmKLCRs in maize were characterized and cloned, and interactions between ZmIQD27 and ZmCaMs, and ZmKLCRs were verified in vitro and in vivo. A ZmCaM-ZmIQD27-ZmKLCR cascade was characterized in maize, which would finally enrich our molecular network of how ZmIQD27 mediates SCW development.

## 1 Materials and Methods

### 1.1 Plant materials

Maize seedlings were maintained at (28±2)°C under a 14 h light (3 500 lux)/10 h dark photoperiod at 70% humidity in a greenhouse.

*Nicotiana benthamiana* plants were grown in a greenhouse at 22°C to 24°C under long-day conditions (16 h of light/8 h of dark).

### 1.2 Gene cloning and vector construction

DNA and amino acid sequences of CaMs and KLCRs in Arabidopsis were obtained by typing gene accession number (Table 1) in TAIR (https://www.arabidopsis.org/index.jsp). BlastN and BlastP were performed in MazieGDB (https://www.arabidopsis.org/index.jsp) to obtain homologous CaMs and KLCRs in maize.

Total RNA was extracted from maize root, electrophoresis was later performed to check RNA quality. RNA was further reverse-transcript into cDNA. Gene-specific primers were used to amplify the coding sequences of ZmIQD27, ZmCaMs, and ZmKLCRs (without terminal codons) with appropriate restriction enzyme sites from cDNA. Primers used in PCR amplifications were listed in Table 1. Amplified fragments were ligated in-frame to the 5'-terminus with the expression vector. Truncated ZmIQD27 (ZmIQD27 I~ZmIQD27 V) were amplified and vectors were constructed as described. Primers used to amplify truncated ZmIQD27 I to V were listed (Table 1).

### 1.3 Sequence alignment and phylogenetic analysis of ZmCaMs and ZmKLCRs

Multi-alignments of ZmCaMs and AtCaM2 in Arabidopsis, ZmKLCRs, and AtKLCR1-3 in Arabidopsis were performed by using MEGA7.0. The phylogenetic trees were constructed by the neighbor-joining (NJ) method using the MEGA7.0 program with Poisson-corrected distances, with 1 000 bootstrap replicates.

### 1.4 Subcellular localization

ZmIQD27, ZmCaMs, and ZmKLCRs were cloned in frame into expression vector driven by *35S* promoter. ZmIQD27, ZmCaMs, and ZmKLCRs were recombined with GFP, thus GFP signals could be traced for subcellular localization. For transient expression assays, *Nicotiana benthamiana* leaves were co-infiltrated with *Agrobacterium tumefaciens* GV3101 pMP90RK harboring plasmids and the silencing suppressor p19 in a 1:1 ratio. Bacterial cultures were adjusted to an optical density of 0.5 at 600 nm using infiltration buffer, and *Nicotiana benthamiana* leaves were pressure-infiltrated through the abaxial epidermis. Transgenic leaves were placed in the dark for more than 48 h and the GFP signal was detected by laser scanning confocal microscopy (Zeiss LSM 800, Oberkochen, Germany).

Table 1 Forward and reverse primers of genes in our study

| Gene name | Gene accession number | Primer sequence-F | Primer sequence-R |
|---|---|---|---|
| IQD27 | GRMZM2G024799 | ATGGGTAAGAAGGGAAATTGGTTCAC | CTTAAAGGACCTCGTGCCG |
| CaM1 | GRMZM2G117582 | ATGGCGGACCAGCTCACC | CTTGGCCATCATAACCTTGACGAACT |
| CaM2 | GRMZM2G067511 | ATGGCGGACCAGCTCACC | CTTGGCCATCATCACCTTCACGAAC |
| CaM3 | GRMZM2G152891 | ATGGCGGACCAGCTCACC | CTTGGCCATCATGACCTTGACG |
| CaM4 | GRMZM2G115628 | ATGGAGGAGGTGGAGCAGCA | CTCCCATGCTCTTCCAGCT |
| CaM5 | GRMZM2G155822 | ATGGGAGGTGTAATTAGTGGTGACTCACC | TTCTTCTTCGTCCTCGTCTTCTTCATTATTGATCC |
| CaM6 | GRMZM2G142693 | ATGGGAGGTATAATTAGTGGGGAC | TTCTTCTTTATCTTCATCATCATCGTCTTC |
| KLCR1 | GRMZM2G147377 | ATGCCTGGAATTACAATGGATGG | TGCAGCAACTGCATTTCTCTTG |
| KLCR2 | GRMZM2G060947 | ATGCCTGGAATTACAGAGGA | TGCAGCAACGGCATTTCTCTT |
| AtCaM2 | At2g41110 | - | - |
| AtKLCR1 | AT4G10840 | - | - |
| AtKLCR2 | AT3G27960 | - | - |
| AtKLCR3 | AT1G27500 | - | - |
| IQD27 I | - | ATGGGTAAGAAGGGAAATTGGTTC | CCGGTAGTTCCGCCGCGCCAT |
| IQD27 II | - | TCGCTGCGCGGGCTGATC | CTACTTAAAGGACCTCGTGCCGA |
| IQD27 III | - | CGCGCGCGCG | CCGGTAGTTCCGCCGCGCCAT |
| IQD27 IV | - | ATGGGTAAGAAGGGAAATTGGTTC | CGCCGCCGGAC |
| IQD27 V | - | CGCGCGCGCG | CTACTTAAAGGACCTCGTGCCGA |
| IQD27 I | - | ATGGGTAAGAAGGGAAATTGGTTC | CCGGTAGTTCCGCCGCGCCAT |

### 1.5 Yeast-two hybridization (Y2H)

To further verify protein-protein interactions, full-length, and truncated ZmIQD27 were amplified and cloned into pGBKT7, ZmCaMs and ZmKLCRs were amplified and cloned into pGADT7, and later verifications were conducted as the manufacturers' instructions. All the sequences of the primers used in the cloning process are given (Table 1).

pGADT7-CaMs/KLCRs was introduced together with pGBKT7-ZmIQD27 (either full length ZmIQD27 or truncated ZmIQD27) into the yeast strain AH109 by cotransformation. The co-transformations were selected on different SD mediums lacking tryptophan (Trp) and Leucine (Leu) (SD/Trp-Leu-) and finally on the SD medium lacking adenine (Ade), His, Trp, and Leu (SD/Trp-Leu-His-Ade-).

### 1.6 Bimolecular Fluorescent Complimentary (BiFc) and immune-fluorescence

The fluorescence signal of the yellow fluorescence protein (YFP) was measured for protein-protein interactions. The open reading frames of ZmIQD27, ZmKLCRs, and ZmCaMs were amplified from Maize cDNA. The amplified open reading frame was inserted into the pUC-SPYCE or pUC-SPYNE vector, driven by the *35S* promoter, and fused to the YFP-N or YFP-C in the frame. Plasmids were transformed into GV3101, and the positive colony was selected for later analysis. The mixtures of the bacterial cultures were incubated, then infiltrated into fully grown upper leaves of a six-week-old *Nicotiana benthamiana*. The YFP signal was detected by laser scanning confocal microscopy (Zeiss LSM 700, Germany). YFP signals would be visualized when there is protein-protein interaction.

### 1.7 Pull-down assay

For pull-down assay, the ZmIQD27 and CaM/KLCR coding regions were cloned into the pET-28b (+) and pGEX-4T-1 vectors, respectively. The recombinant 6×His-ZmIQD27 and GST-CaMs/KLCRs proteins were purified using amylose resin (Yeasen) and Ni-NTA sefinose resin (Smart-Lifesciences). GST-CaMs/KLCRs or GST protein alone was immobilized with amylose resin and incubated with 6×His-ZmIQD27 in incubation buffer under gentle agitation. After being washed five times, 1×SDS loading buffer was added into the bead-retained protein and boiled for 5 min, followed by analyzing in 12% SDS-PAGE, then visualization by Western blot assay with anti-GST and anti-6×His antibodies.

## 2 Results

### 2.1 Identification of CaMs and KLCRs in maize

To characterize the homozygous CaMs and KLCRs in maize, DNA and amono acid sequences of CaMs and KLCRs in Arabidopsis were obtained by typing gene number (Table 1) in TAIR (https://www.arabidopsis.org/index.jsp). BlastN and BlastP were performed in MazieGDB to obtain homozygous CaMs and KLCRs in maize. As a result, six CaMs, named CaM1-6, were found in maize (Table 1). ZmCaM1-3 has 149 amino acids in total. Amino acids sequences of ZmCaMs were aligned. Sequence identity either between CaM1 and CaM2, or between CaM2 and CaM3, was 99.0% (Figure 1A; Figure 1C). Sequence identity between CaM1 and CaM3 was 98.65%. ZmCaM5 and ZmCaM6 have 187 amino acids. The sequence identity between CaM5 and CaM6 was 93.02%. The expression level of ZmCaM4 identified in the MaizeGDB database was low in general. Since a high level of sequence similarity, we select and cloned ZmCaM2, ZmCaM3, ZmCaM5, and ZmCaM6 respectively for later analyses.

Two KLCRs, named ZmKLCR1 and ZmKLCR2, were found in maize by using the CDS sequence of AtKLCR1 as a query (Table 1). The identity of amino acid sequences for ZmKLCR1 and ZmKLCR2 was 94.53% (Figure 1B; Figure 1D). ZmKLCR1 and ZmKLCR2 were cloned for later analyses.

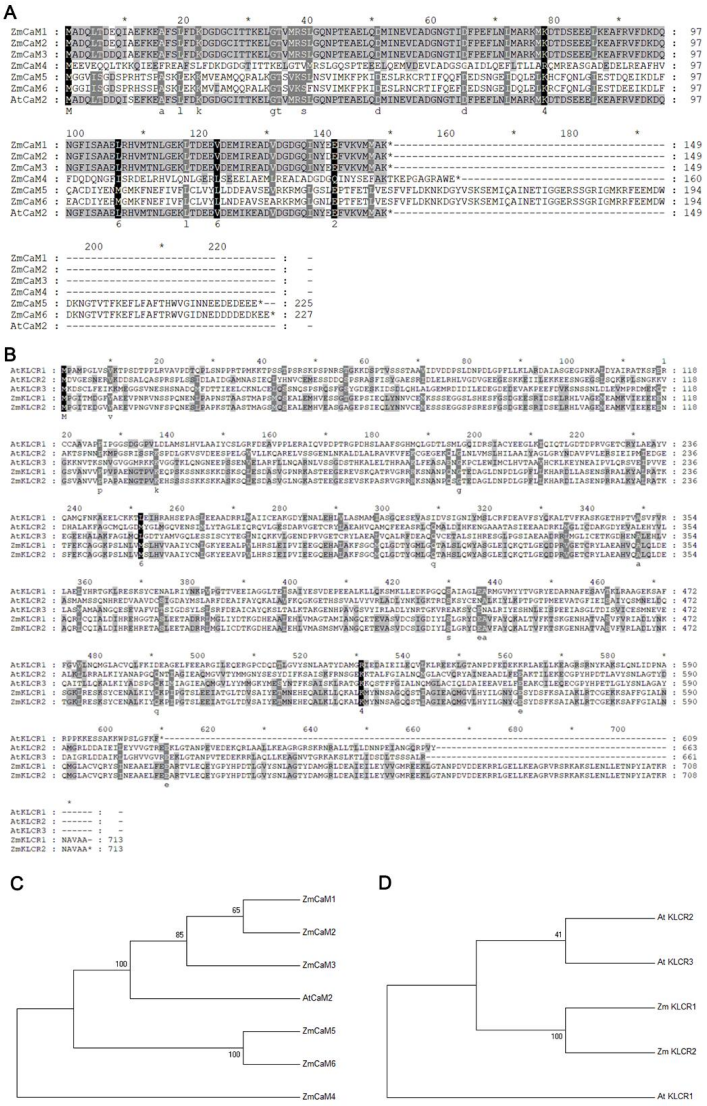


Figure 1 Sequence alignment of CaMs and KLCRs in maize and Arabidopsis

Note: A: Amino acid sequence alignments of ZmCaM1-6 and AtCaM2; B: Amino acid sequence alignments of ZmKLCR1-2 and AtKLCR1-3; C: A phylogenetic tree of ZmCaM1-6 and AtCaM2; D: A phylogenetic tree of ZmKLCR1-2 and AtKLCR1-3

### 2.2 Subcellular localization

To gain insights into the cellular sites of ZmIQD27, ZmCaMs, and ZmKLCRs, we studied the subcellular distribution of those proteins after transient expression in *Nicotiana benthamiana* leaves, which is a convenient system in which to monitor protein localization (Deeks et al., 2012). The GFP-tagged CaM2, CaM3, CaM5, and CaM6 were found in the cell membrane, cell cytoplasm, and cell nuclear (Figure 2). The GFP-tagged ZmIQD27 expression vector was transformed into *Nicotiana benthamiana* leaves. GFP signals were visualized at cortical microtubules (Figure 3B), which was consistent with our previous results (Li et al., In press). GFP-integrated KLCR1 and KLCR2 were visualized in the cell cytoplasm and cell membrane (Figure 3C; Figure 3D). The subcellular localizations of ZmCaMs and ZmKLCRs were consistent with their putative cellular functions.

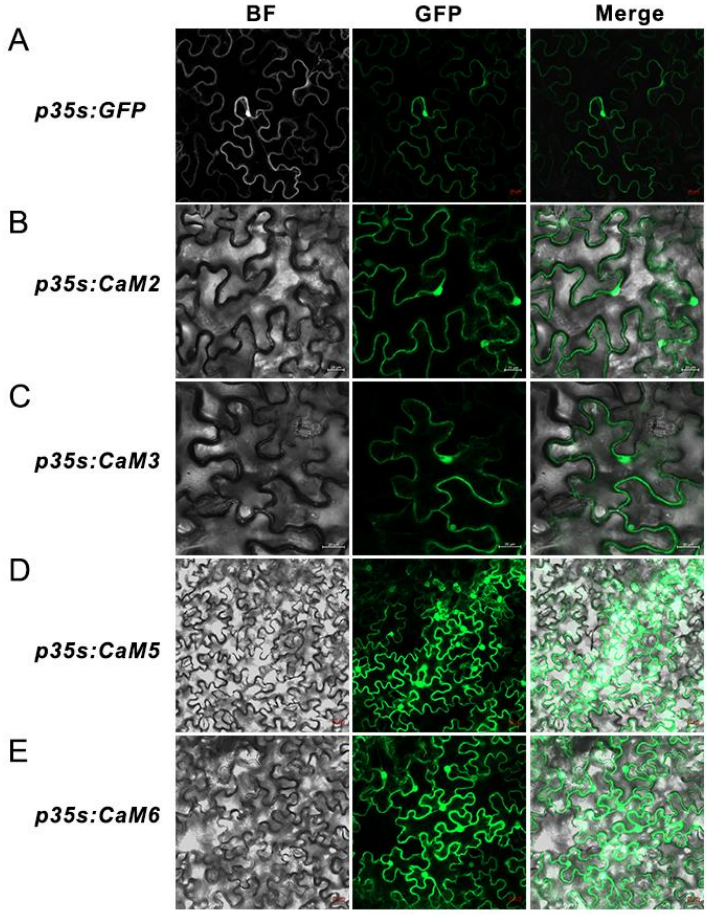


Figure 2 Subcellular localization of ZmCaMs

Note: A: Subcellular localization of GFP expression vector driven by *35s* promoter; B: Subcellular localization of GFP tagged CaM2; C: Subcellular localization of GFP tagged CaM3; D: Subcellular localization of GFP tagged CaM5; E: Subcellular localization of GFP tagged CaM6; BF: Bright field; GFP: Green fluorescent protein; Scale bars=20 μm

### 2.3 ZmIQD27 interacts with ZmCaMs, and ZmKLCRs *in vivo*

ZmIQD27 are typically signal proteins that bind to CaM. In Arabidopsis, IQDs act as scaffold proteins and mediate cell wall formation via KLCR. To validate in vivo interactions of ZmIQD27 with ZmCaMs and ZmKLCRs, we performed yeast two-hybrid interaction (Y2H) assays. Full-length ZmIQD27 was amplified from cDNA by using the primers (Table 1). Four ZmCaMs (ZmCaM2-3, ZmCaM5-6) and two ZmKLCRs (ZmKLCR1 and ZmKLCR2) were cloned and ligated to pGADT7 vector. ZmIQD27 was ligated to the pGBKT7 vector. As a result, interactions were found between ZmIQD27 and ZmCaM2, ZmCaM3, ZmKLCR1, and ZmKLCR2, while no interaction was found with ZmCaM6 and ZmCaM5 (Figure 4B).

Interaction between ZmIQD27 and ZmCaM2, ZmCaM3, ZmKLCR1, and ZmKLCR2 were further verified by BiFC (Figure 4C). YFP signals were visualized at the cell membrane and cell cytoplasm, indicating their

interactions at the cell membrane and cell cytoplasm. It is noteworthy that ZmCaM2 locates in the cytoplasm, when cotransformed into *Nicotiana benthamiana* leaves with ZmIQD27, YFP signals were visualized at microtubules, indicating the recruitment of ZmCaM2 to the microtubular network by ZmIQD27.

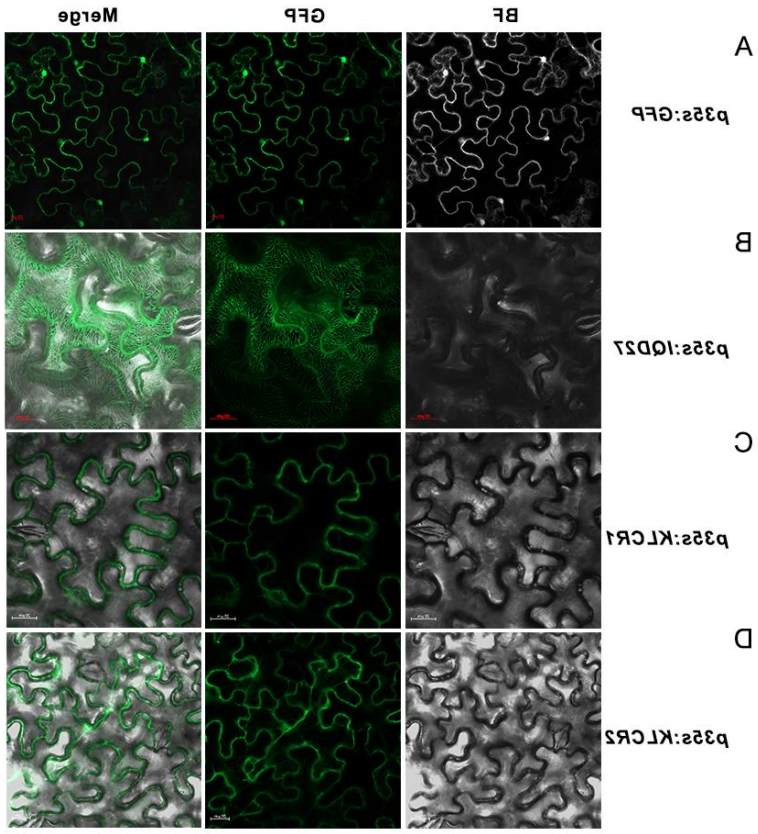


Figure 3 Subcellular localization of ZmIQD27 and ZmKLCRs

Note: A: Subcellular localization of GFP expression vector driven by 35s promoter; B: Subcellular localization of GFP tagged IQD27; C: Subcellular localization of GFP tagged KLCR1; D: Subcellular localization of GFP tagged KLCR2; BF: Bright field; GFP: Green fluorescent protein; Scale bars=20 μm

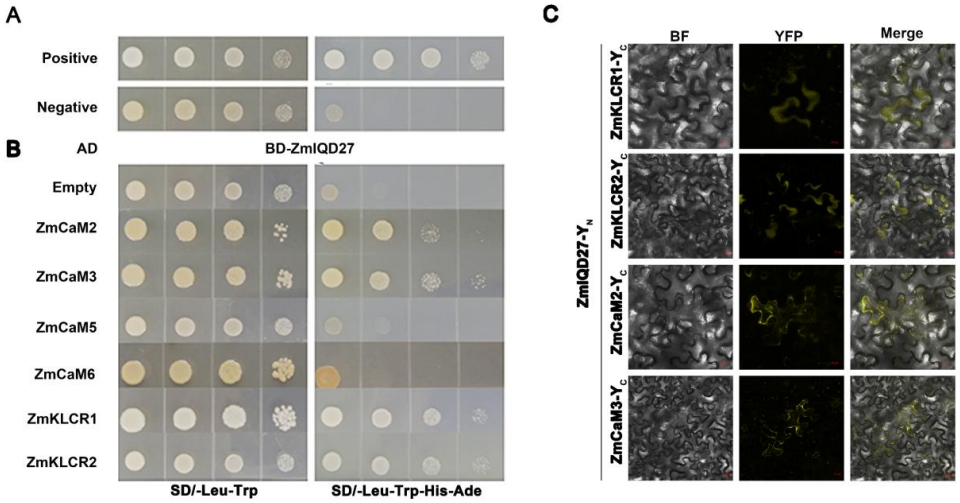


Figure 4 Protein-protein interactions between ZmIQD27 and ZmKLCRs, ZmCaMs *in vivo*

Note: A: Positive and negative controls of Y2H analysis, Vectors pGBKT7 (BD) and pGADT7 (AD) were used as negative controls, and vectors pGBKT7-53 and pGADT7-T were used as positive controls; B: Y2H analyses, interaction is indicated by the ability of cells to grow on a dropout medium lacking Leu, Trp, His, and Ade; C: BiFC analyses, Fluorescence was observed in the nuclear compartment of transformed cells, which resulted from the complementation of the C-terminal region of YFP fused with ZmKLCRs or ZmCaMs with the N-terminal region of YFP fused with ZmIQD27, Scale bars=20 μm

### 2.4 ZmIQD27 interacts with ZmCaMs, ZmKLCRs *in vitro*

To confirm the interaction between ZmIQD27 and ZmCaMs, ZmKLCRs *in vitro*, a pull-down assay was performed. The full-length ZmIQD27 was expressed with 6×His tag in *E*. coli, and the 6×His-ZmIQD27 recombinant proteins were purified using amylose resin and Ni-NTA sense resin. ZmCaMs and ZmKLCRs were expressed in *E*. coli as a GST tag recombinant protein. Purified ZmCaMs/KLCRs-GST or GST alone was incubated with bead-bound 6×His-ZmIQD27 fusion protein. The recombinant protein ZmIQD27-6×His interacts with ZmCaM2/3/5/6-GST interacts but not with GST alone (Figure 5A; Figure 5B; Figure 5C; Figure 5D). The recombinant protein ZmIQD27-6×His interacts with ZmKLCR1/2-GST interacts but not with GST alone (Figure 5E; Figure 5F).

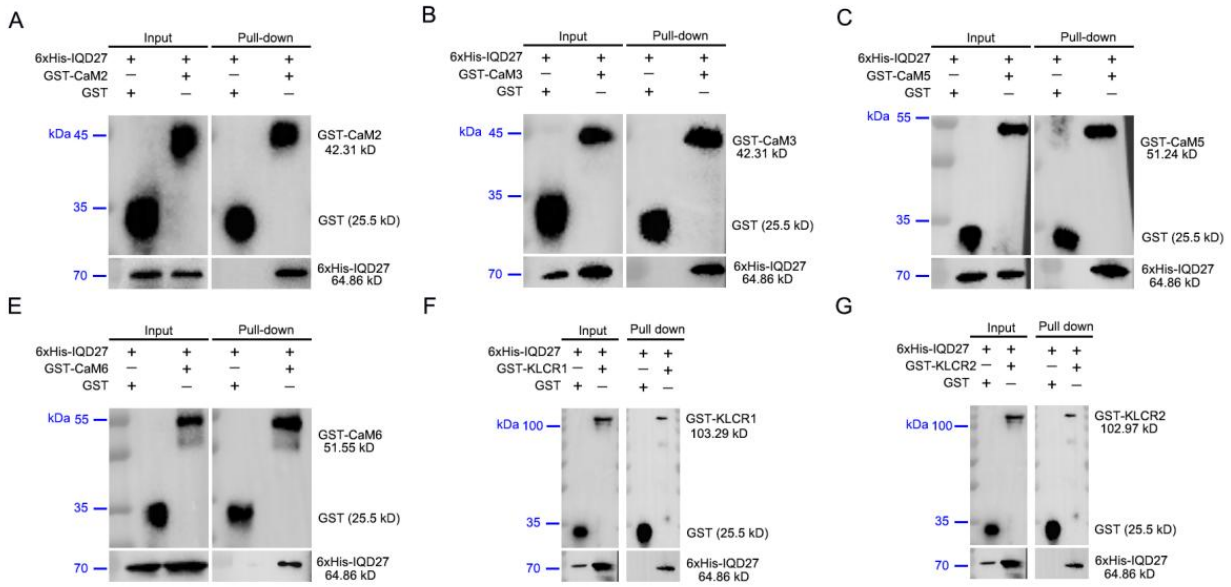


Figure 5 Pull-down assays for interactions between ZmIQD27 and ZmKLCRs, ZmCaMs

Note: A: Pull-down assay for interactions between ZmIQD27 and ZmCaM2; B: Pull-down assay for interactions between ZmIQD27 and ZmCaM3; C: Pull-down assay for interactions between ZmIQD27 and ZmCaM5; D: Pull-down assay for interactions between ZmIQD27 and ZmCaM6; E: Pull-down assay for interactions between ZmIQD27 and ZmKLCR1; F: Pull-down assay for interactions between ZmIQD27 and ZmKLCR2; Equal amounts of GST-ZmCaMs/KLCRs and GST were combined with anti-GST magnetic beads preincubated with 6×His-ZmIQD27, Pulled-down samples were analyzed by immunoblot with anti-GST and anti-6×His antibodies. "+" and "–" indicate the presence and absence of corresponding proteins in the reactions, respectively, GST: Glutathione S-Transferase

### 2.5 ZmIQD27 motif responsible for binding CaMs and KLCRs

To further clarify the motif that is responsible for binding CaMs and KLCRs, respectively, full length ZmIQD27 were truncated into I ~V (Figure 6). The total length of *ZmIQD27* was 1 683 bp. ZmIQD27 has 561 amino acids in which there is an IQD domain ranges from 209 to 231. Truncated ZmIQD27 I (1 to 231), III (209 to 231) and V (209 to 561), contained IQD domain. I and V interacted with ZmCaM2 and ZmCaM3, as well asl KLCR1 (Figure 6E; Figure 6I). III interacted with ZmCaM2 and ZmCaM3 (Figure 6G). Truncated ZmIQD27 II (231 to 561) interacted with KLCR1 and KLCR2. IV (1 to 209) interacted with KLCR1. Based on these results, we summarized that IQ domain was responsible for binding CaMs, which was as expected; KLCR1 can binds with the motif either at the N terminal and C terminal fragments divided by IQ domain. The motif that responsible for KLCR2 binding needs a further study.

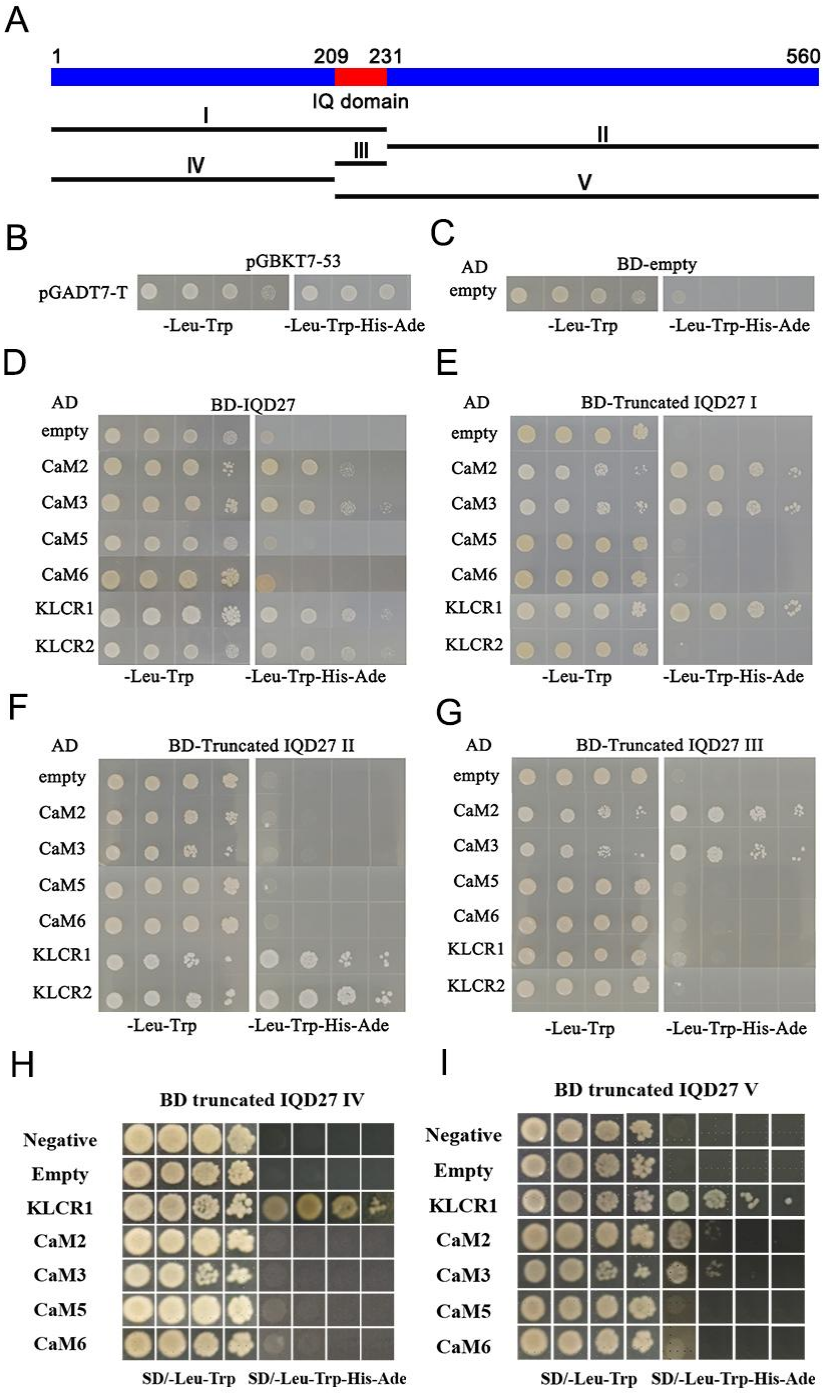


Figure 6 Truncated ZmIQD27s interact with ZmCaMs and ZmKLCRs

Note: A: Schematic diagram of the truncated ZmIQD27, named as I, II, III, IV, and V used in this experiment; B: Positive controls of Y2H analysis; C: Negative control of Y2H analysis; D: Y2H analysis between full-length ZmIQD27 and ZmCaMs and ZmKLCRs; E: Y2H analysis between truncated ZmIQD27 I and ZmCaMs and ZmKLCRs; F: Y2H analysis between truncated ZmIQD27 II and ZmCaMs and ZmKLCRs; G: Y2H analysis between truncated ZmIQD27 III and ZmCaMs and ZmKLCRs; H: Y2H analysis between truncated ZmIQD27 IV and ZmCaMs and ZmKLCRs; I: Y2H analysis between truncated ZmIQD27 V and ZmCaMs and ZmKLCRs

## 3 Discussion

Screening from an EMS mutant library of maize B73, a drought-sensitive like mutant was characterized previously in our lab (Li et al., 2023). The causal gene of the mutant was *ZmIQD27*. ZmIQD27 colocalized with microtubules, its mutation resulted in a microtubular orientated SCW deposition defect (Li et al., 2023). The detailed molecular mechanism of how ZmIQD27 modulates microtubule arrangement remain unclear. In our study,

a ZmCaMs-ZmIQD27-ZmKLCRs cascade would contribute to the underline molecular mechanism of how ZmIQD27 mediates microtubule arrangement.

IQD protein is a class of calmodulin-binding proteins, interactions between IQD protein and CaM were verified in Arabidopsis (Bürstenbinder et al., 2013), however, there is no relevant report in maize. Published AtCaM, AtKLCR and their interactions with AtIQD1 protein in Arabidopsis (Bürstenbinder et al., 2013) offer a research basis to conduct our study. Four CaMs and 2 KLCRs were cloned after homozygous alignments with CaM and KLCR in Arabidopsis. A high level of sequence similarity of CaM and KLCRs between that in Arabidopsis and that in Maize, indicating the sequence and functions of CaMs and KLCRs would be conserved in Arabidopsis and Maize. In Arabidopsis, there are interactions between IQD and CMLs, which were not included in our analysis. Further analysis including CaM and CML is necessary to uncover the interactions between IQD27 and its interacting proteins.

In Arabidopsis, recruitment of KLCR1 from cytoplasm localization to microtubules by IQD1 was found (Bürstenbinder et al., 2013). In our BiFC assay, recruitment from the cytoplasm to microtubules was visualized when ZmCaM2, not ZmKLCR1 or ZmLLCR2, was cotransformed with ZmIQD27, although ZmKLCR1 and KLCR2 interact with ZmIQD27. A further functional study of ZmKCLR1 and ZmKLCR2 is necessary to give a full explanation of the molecular mechanism of ZmIQD27 in mediating SCW development.

Summary from our results, a model of ZmIQD27 acts as a scaffold that mediates vesicle from Golgi to the cell membrane was proposed. ZmIQD27 integrates signals via interaction with ZmCaMs and later guides the microtubule-guided and kinesin-dependent vesicle transportation from Golgi to the cell membrane (Figure 7).

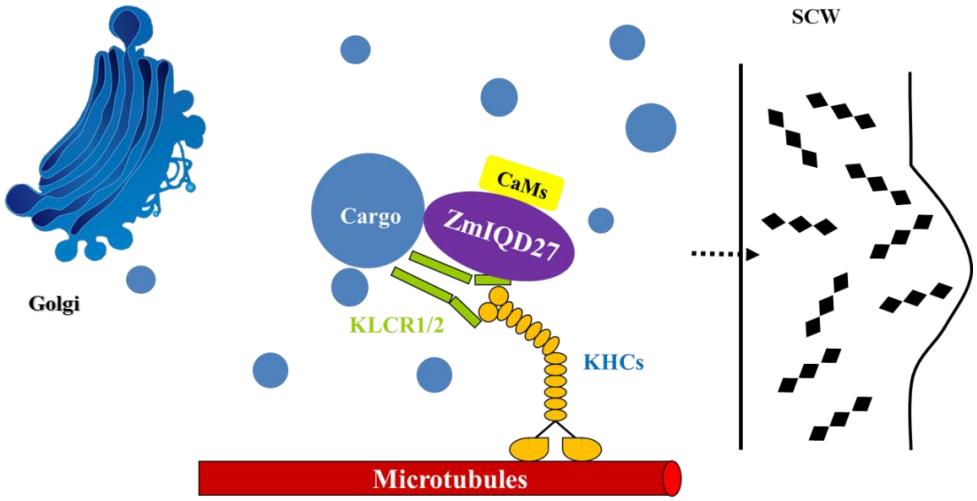


Figure 7 A proposed model for how ZmIQD27 mediates cell wall development via microtubules

Note: ZmIQD27 is proposed to function as a scaffold protein that likely recruits various cargos to kinesins (KHCs) via associated KLCR1 or KLCR2 for unidirectional transport along microtubule tracks, transport cargos are currently

## Authors' contributions

Gao Yongmeng performed almost all the experiments, Xie Jun helped in parts of the Y2H and sub-cellular localization observations. Lu Xiaoduo and Haiyan Li arranged all the experiments, Lu Xiaoduo offered constructive suggestions and Haiyan Li wrote the manuscript.

## Acknowledgements

We acknowledgement all the members in our lab for help and discussions.

## References

Abel S., Bürstenbinder K., and Müller J., 2013, The emerging function of IQD proteins as scaffolds in cellular signaling and trafficking, Plant Signal Behav., 8: e24369.
https://doi.org/10.4161/psb.24369
PMid:23531692 PMCid:PMC3909082

Abel S., Savchenko T., and Levy M., 2005, Genome-wide comparative analysis of the IQD gene families in Arabidopsis thaliana and Oryza sativa, BMC Evol. Biol., 5: 72.
https://doi.org/10.1186/1471-2148-5-72
PMid:16368012 PMCid:PMC1368998

Badmi R., Payyavula R.S., Bali G., Guo H.B., Jawdy S.S., Gunter L.E., Yang X., Winkeler K.A., Collins C., Rottmann W.H., Yee K., Rodriguez M.J., Sykes R.W., Decker S.R., Davis M.F., Ragauskas A.J., Tuskan G.A., and Kalluri U.C., 2018, A new calmodulin-binding protein expresses in the context of secondary cell-wall biosynthesis and impacts biomass properties in Populus, Front Plant Sci., 9: 1669.
https://doi.org/10.3389/fpls.2018.01669
PMid:30568662 PMCid:PMC6290091

Bi L., Weng L., Jiang Z., and Xiao H., 2018, The tomato IQD gene SUN24 regulates seed germination through ABA signaling pathway, Planta, 248: 919-931.
https://doi.org/10.1007/s00425-018-2950-6
PMid:29968062

Bürstenbinder K., Mitra D., and Quegwer J., 2017a, Functions of IQD proteins as hubs in cellular calcium and auxin signaling: A toolbox for shape formation and tissue-specification in plants? Plant Signal Behav., 12: e1331198.
https://doi.org/10.1080/15592324.2017.1331198
PMid:28534650 PMCid:PMC5566250

Bürstenbinder K., Möller B., Plötner R., Stamm G., Hause G., Mitra D., and Abel S., 2017b, The IQD family of calmodulin-binding proteins links calcium signaling to microtubules, membrane subdomains, and the nucleus, Plant Physiol., 173: 1692-1708.
https://doi.org/10.1104/pp.16.01743
PMid:28115582 PMCid:PMC5338658

Bürstenbinder K., Savchenko T., Müller J., Adamson A.W., Stamm G., Kwong R., Zipp B.J., Dinesh D.C., and Abel S., 2013, Arabidopsis calmodulin-binding protein IQ67-domain 1 localizes to microtubules and interacts with kinesin light chain-related protein-1, J. Biol. Chem., 288: 1871-1882.
https://doi.org/10.1074/jbc.M112.396200
PMid:23204523 PMCid:PMC3548496

Cai R., Zhang C., Zhao Y., Zhu K., Wang Y., Jiang H., Xiang Y., and Cheng B., 2016, Genome-wide analysis of the IQD gene family in maize, Mol. Genet. Genomics, 291: 543-558.
https://doi.org/10.1007/s00438-015-1122-7
PMid:26453258

Deeks M.J., Calcutt J.R., Ingle E.K.S., Hawkins T.J., Chapman S., Richardson A.C., Mentlak D.A., Dixon M.R., Cartwright F., and Smertenko A.P., 2012, A superfamily of actin-binding proteins at the actin-membrane nexus of higher plants, Curr. Biol., 22: 1595-1600.
https://doi.org/10.1016/j.cub.2012.06.041
PMid:22840520

Feng L., Chen Z., Ma H., Chen X., Li Y., Wang Y., and Xiang Y., 2014, The IQD gene family in soybean: structure, phylogeny, evolution and expression, PLoS One, 9: e110896.
https://doi.org/10.1371/journal.pone.0110896
PMid:25343341 PMCid:PMC4208818

Li H., Xie J., Gao Y., Wang X., Qin L., Ju W., Roberts J.A., Cheng B., Zhang X., and Lu X., 2023, IQ domain-containing protein ZmIQD27 modulates water transport in maize, Plant physiology, kiad390. Advance online publication.
https://doi.org/10.1093/plphys/kiad390
PMid:37403650

Li Y., Huang Y., Wen Y., Wang D., Liu H., Li Y., Zhao J., An L., Yu F., and Liu X., 2021, The domain of unknown function 4005 (DUF4005) in an Arabidopsis IQD-protein functions in microtubule binding, J. Biol. Chem., 297: 100849.
https://doi.org/10.1016/j.jbc.2021.100849
PMid:34058197 PMCid:PMC8246641

Liu Z., Haider M.S., Khan N., and Fang J., 2020, Comprehensive sequence analysis of IQD gene family and their expression profiling in Grapevine (Vitis vinifera), Genes (Basel), 11: 235.
https://doi.org/10.3390/genes11020235
PMid:32102395 PMCid:PMC7073947

Lu X., Liu J., Ren W., Yang Q., Chai Z., Chen R., Wang L., Zhao J., Lang Z., Wang H., Fan Y., Zhao J., and Zhang C., 2018, Gene-indexed mutations in maize, Mol. Plant, 11: 496-504.
https://doi.org/10.1016/j.molp.2017.11.013
PMid:29223623

Ma H., Feng L., Chen Z., Chen X., Zhao H., and Xiang Y., 2014, Genome-wide identification and expression analysis of the IQD gene family in Populus trichocarpa, Plant Sci., 229: 96-110.
https://doi.org/10.1016/j.plantsci.2014.08.017
PMid:25443837

Mei C., Liu Y., Dong X., Song Q., Wang H., Shi H., and Feng R., 2021, Genome-wide identification and characterization of the potato IQD family during development and stress, Front Genet., 12: 693936.
https://doi.org/10.3389/fgene.2021.693936
PMid:34386041 PMCid:PMC8354571

Mitra D., Klemm S., Kumari P., Quegwer J., Möller B., Poeschl Y., Pflug P., Stamm G., Abel S., and Bürstenbinder K., 2019, Microtubule-associated protein IQ67 DOMAIN5 regulates morphogenesis of leaf pavement cells in Arabidopsis thaliana., J. Exp. Bot., 70: 529-543.
https://doi.org/10.1093/jxb/ery395
PMid:30407556 PMCid:PMC6322583

Oda Y., and Fukuda H., 2012, Secondary cell-wall patterning during xylem differentiation, Curr. Opin. Plant Biol., 15: 38-44.
https://doi.org/10.1016/j.pbi.2011.10.005
PMid:22078063

Oda Y., and Fukuda H., 2013a, Spatial organization of xylem cell-walls by ROP GTPases and microtubule-associated proteins, Curr. Opin. Plant Biol., 16: 743-748.
https://doi.org/10.1016/j.pbi.2013.10.010
PMid:24210792

Oda Y., and Fukuda H., 2013b, Rho of plant GTPase signaling regulates the behavior of Arabidopsis kinesin-13A to establish secondary cell-wall patterns, Plant Cell, 25: 4439-4450.
https://doi.org/10.1105/tpc.113.117853
PMid:24280391 PMCid:PMC3875728

Oda Y., and Hasezawa S., 2006, Cytoskeletal organization during xylem cell differentiation, J. Plant Res., 119: 167-177.
https://doi.org/10.1007/s10265-006-0260-8
PMid:16570127

Oda Y., Iida Y., Kondo Y., and Fukuda H., 2010, Wood cell-wall structure requires local 2D-microtubule disassembly by a novel plasma membrane-anchored protein, Curr. Biol., 20: 1197-1202.
https://doi.org/10.1016/j.cub.2010.05.038
PMid:20619818

Sugiyama Y., Wakazaki M., Toyooka K., Fukuda H., and Oda Y., 2017, A novel plasma membrane-anchored protein regulates xylem cell-wall deposition through microtubule-dependent lateral inhibition of Rho GTPase domains, Curr. Biol., 27: 2522-2528.
https://doi.org/10.1016/j.cub.2017.06.059
PMid:28803875

Wu M., Li Y., Chen D., Liu H., Zhu D., and Xiang Y., 2016, Genome-wide identification and expression analysis of the IQD gene family in moso bamboo (Phyllostachys edulis), Sci. Rep., 6: 24520.
https://doi.org/10.1038/srep24520
PMid:27094318 PMCid:PMC4837358

Yuan J., Liu T., Yu Z., Li Y., Ren H., Hou X., and Li Y., 2019, Genome-wide analysis of the Chinese cabbage IQD gene family and the response of BrIQD5 in drought resistance, Plant Mol. Biol., 99: 603-620.
https://doi.org/10.1007/s11103-019-00839-5
PMid:30783953